Journal of Particle Science and Technology 10 (2) (2024) 109-115

Iranian Research Organization for Science and Technology (IROST)

Journal of PARTICLE Science & Technology

JPSIT
https://jpst.irost.ir

Online ISSN: 2423-4079
Print ISSN: 2423-4087

Synthesis and investigation of photocatalytic properties of $CaSnO_3$/Ag composite

Sayed Ali Hassanzadeh-Tabrizi✉

Advanced Materials Research Center, Department of Materials Engineering, Na.C, Islamic Azad University, Najafabad, Iran

HIGHLIGHTS

- $CaSnO_3$/Ag were synthesized via a hydrothermal route as a new photocatalyst.
- The hybrid material shows higher photocatalytic activity for photodegradation.
- Coupling $CaSnO_3$ with Ag endowed the photocatalysts with a higher kinetic rate constant.

GRAPHICAL ABSTRACT

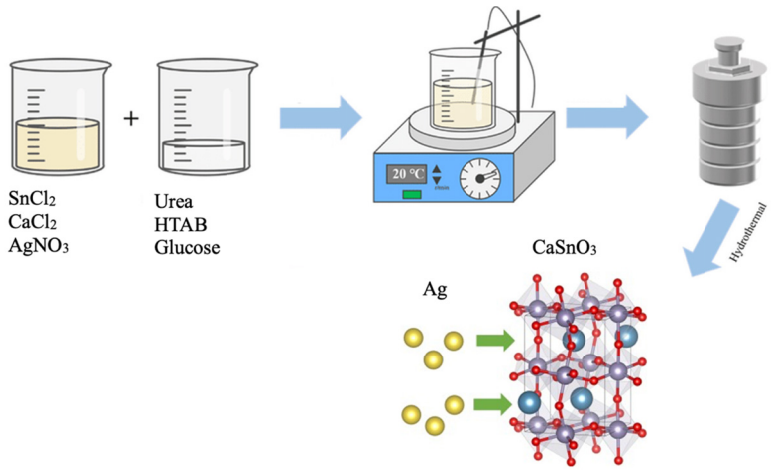

ARTICLE INFO

Article type:

Research article

Article history:

Received 11 February 2025
Received in revised form 15 March 2025
Accepted 13 April 2025

Keywords:

Ag
$CaSnO_3$
Photocatalyst
Methyl orange
Decolorization

ABSTRACT

Environmental crises, including polluted waters and the emission of greenhouse gases, have been major problems for societies in recent years. As a result, the need for innovative purification systems has recently become one of the main research fields. Photocatalysts are recognized as one of the prominent methods for the removal and degradation of pollutants. These techniques are particularly effective in reducing organic pollutants in wastewater. In the present study, a $CaSnO_3$/Ag photocatalytic system was synthesized using the hydrothermal method. X-ray diffraction (XRD) and scanning electron microscopy (SEM) techniques were employed to identify the produced photocatalytic system. The Williamson-Hall method was used to measure the crystallite size and lattice strain. The photocatalytic activity of the synthesized material was investigated using the degradation of the organic dye methyl orange. The results of XRD analysis indicated the formation of two phases: calcium stannate with a perovskite structure and silver with a cubic crystal structure. The particle size distribution of the produced particles was uniform, with most particles ranging between 100 and 250 nm. The particles precipitated in the hydrothermal container had a spherical shape. The photocatalytic degradation of calcium stannate samples increased after combining with silver. The kinetic rate constant obtained for the degradation of methyl orange for pure calcium stannate and the composite sample was 0.004 and 0.007, respectively.

DOI: 10.22104/jpst.2025.7413.1272

✉ *Corresponding author: E-mail address:* hassanzadeh@iau.ac.ir ; *Tel:* +9831-42292893

1. Introduction

With the development of industrial processes, environmental pollution, especially water pollution, has become a major problem. Water resources are limited in countries and human societies, resulting in a great need for water recycling and reuse in agriculture and industry. Given the fact that industrial wastewaters have a high concentration of organic matter, they cannot be easily treated by conventional methods. For instance, the removal of azo dyes such as methyl orange is difficult using conventional biological and/or physicochemical treatments. Methyl orange is widely used in the dyeing, leather, textile, paper, and printing industries, as well as in research laboratories, and is a major component of many industrial waste discharges, causing pollution of various water resources. These dyes can cause cell mutation, cancer, and toxicity to organisms. Its excessive presence in drinking water can also cause anemia, abdominal pain, headache, dizziness, confusion, excessive sweating, and nausea [1,2].

Solar energy has received much attention in recent years as an accessible and inexpensive resource and can be used as a source for photocatalytic activities in contaminated waters. This process may be economically and technologically feasible for water purification and wastewater decontamination. Photocatalysis is a potential technology for degrading organic pollutants in water, such as aromatic compounds [3]. These organic compounds are considered a potential hazard to the environment. Reactive active radicals carry out oxidation of organic compounds in aqueous solution. Various recently developed nanomaterials, such as nanoparticles, nanowires, nanotubes, nanoporous materials, and hollow materials, have many applications in energy and environmental sciences. Such nanomaterials offer high surface area, fast charge transfer, and selective chemical transformations [4-6].

Alkaline earth stannates have attracted the attention of researchers due to their advantages such as low chemical toxicity, environmental compatibility, suitable optical properties, and chemical and thermal stability. The optical properties, excellent resistance to chemical damage, high mechanical strength, and semiconducting properties of calcium stannate ($CaSnO_3$) make it a suitable semiconductor for photocatalytic applications [7]. Therefore, research has been carried out to improve the photocatalytic properties of this material. For example, doping and attaching other semiconductors to this material have been shown to improve photocatalytic properties [8-13]. Hosseini *et al.* produced $CaSnO_3$/*g*-C_3N_4 (CSO/CN) using a co-precipitation method aided by ultrasound [10]. The ability of CSO, CN, and various CSO/CN nanocomposites to degrade Erythrosine (ER) and Eriochrom Black T was examined. The results showed that the kind of dye, the amount of CSO, the amount of catalyst, and the concentration of ER all impacted the degradation rate. The CSO/CN nanocomposite also showed higher efficiency than pure CSO and CN.

Rakesh *et al.* introduced an innovative heterostructure material combining $CaSnO_3$ perovskite with bismuth tungstate (Bi_2WO_6) [13]. The $CaSnO_3$ component was fabricated through com bustion synthesis, while Bi_2WO_6 was prepared via hydrothermal processing. This hybrid material demonstrates dual functionality, targeting both environmental remediation through UV-driven photocatalytic decomposition of methylene blue (MB) and analytical applications via electrochemical nitrite detection. Under ultraviolet irradiation, the $CaSnO_3$/Bi_2WO_6 system achieved 92.5 % elimination of the environmentally persistent and carcinogenic MB dye within 180 min. Notably, the nanocomposite demonstrated exceptional stability against photo-corrosion, maintaining photocatalytic efficiency even under alkaline conditions (pH = 11) – a critical advantage for practical wastewater treatment applications.

In another research, calcium tin oxide was selected as the base material, and its photocatalytic efficacy was significantly enhanced by incorporating varying proportions of silver silicate ($Ag_6Si_2O_7$) to form a heterostructured composite [13]. The integration of $Ag_6Si_2O_7$ into the $CaSnO_3$ matrix not only facilitated improved charge carrier separation but also enhanced visible light absorption by reducing the optical bandgap. The presence of $Ag_6Si_2O_7$ in the composite catalyst augmented electrical conductivity, thereby effectively directing a substantial portion of the energy to the catalyst surface. Upon evaluating the photocatalytic activity of the $Ag_6Si_2O_7$/$CaSnO_3$ composite against Rhodamine B (RhB) degradation, a remarkable degradation efficiency of 95.24 % was achieved within 60 min. This was accompanied by a degradation rate constant of 0.04971 min^{-1}, which was found to be 24.48 times greater than that of its counterparts.

Noble metals, especially silver (Ag), have a high potential to increase the photocatalytic efficiency of semiconductors due to their high stability, easy preparation, and inherent antibacterial activity. Due to its localized surface plasmon resonance (LSPR) property, silver metal can lead to an interaction between visible light and the metal. This material has been widely used to improve the photocatalytic properties of various semiconductors [14-16].

To the best of our knowledge, there are a few works on investigating the photocatalytic properties of calcium stannate synthesized with noble metals. Therefore, the purpose of this research is to create a composite of calcium stannate and the noble metal silver to increase the catalytic activity of $CaSnO_3$. The hydrothermal method was used for this purpose. Various methods were used to characterize the

synthesized composite, and then its ability to degrade methyl orange dye was evaluated.

2. Experimental

2.1. Materials and methods

A calcium stannate-silver composite was prepared using the hydrothermal method. For this purpose, an equal molar ratio of calcium nitrate (Merck Company) and tin nitrate (Merck Company) was initially poured into a container containing distilled water and stirred until the materials were completely dissolved. Then, silver nitrate (Sigma Aldrich) was added to the solution. Another solution of urea (Dr. Majalli Chemical Industries) in distilled water was prepared. The molar ratio of urea to metal nitrates was 6 to 1. Glucose was also added to the solution for better reduction of the silver ion, and hexadecyl trimethyl ammonium bromide (HTAB) was added as a surfactant. This solution was mixed with the first solution. The resulting sample was transferred to a hydrothermal vessel made of polyethylene. The hydrothermal system was maintained at 200 °C for 5 h. After the reaction was completed, the produced powder was washed with distilled water and ethanol. The product was then collected and dried at 90 °C. The synthesis steps are shown in Fig. 1.

2.2. Characterization

The produced powder was examined using XRD analysis with a Philips X'Pert model device. The morphology and dimensions of the powder were examined using a CamScan MV2300 scanning electron microscope. The samples were coated with a thin layer of gold for scanning electron microscope imaging. ImageJ software was used to analyze the SEM results and measure particle size distribution.

2.3. Measurement of photocatalytic activity

The photocatalytic properties of the produced photocatalyst were measured using the degradation of methyl orange dye in a chamber equipped with two 350 W xenon lamps. In each step, a certain amount of the samples were immersed in 50 ml of methyl orange solution and stirred continuously. Then, the chamber was irradiated at various times, and the dye solution was centrifuged and subjected to UV-Vis spectroscopy for analysis. The measured wavelength was λ = 506 nm. The degradation rate (R) was calculated using Eq. (1).

$$R = (C_0\text{-}C_t) \times 100 / C_0 \quad (1)$$

where C_0 is the initial concentration of methyl orange and C_t refers to the concentration of methyl orange at time t.

3. Results and discussion

After the fabrication process, the synthesis product was analyzed by XRD to examine the formed phases, and the results are shown in Fig. 2. As can be seen, the sample has peaks related to crystalline phases. These peaks indicate the formation of the $CaSnO_3$ phase, which corresponds to International Centre for Diffraction Data (ICDD) card number 001-0998 and indicates an orthorhombic crystal system. This structure consists of SnO6 octahedra, with calcium cations located in the octahedral cavities. The silver peaks appeared at angles of 38°, 44°, and 64°, which correspond to JCPDS card number 01-087-0597 with a cubic crystal system of Ag.

The Williamson-Hall Eq. (2) was used to calculate the size of the crystallites and the lattice strain in the manufactured product [17].

$$\beta cos\theta = 4\varepsilon sin\theta + \frac{0.9\lambda}{d} \quad (2)$$

where d is the crystal size, ε is the lattice strain, λ is the

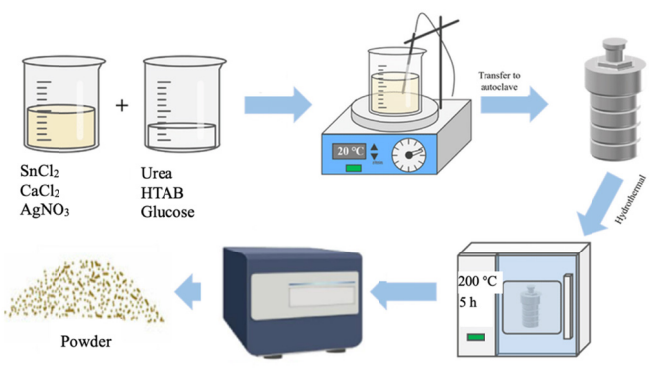

Fig. 1. Synthesis procedure of $CaSnO_3$/Ag.

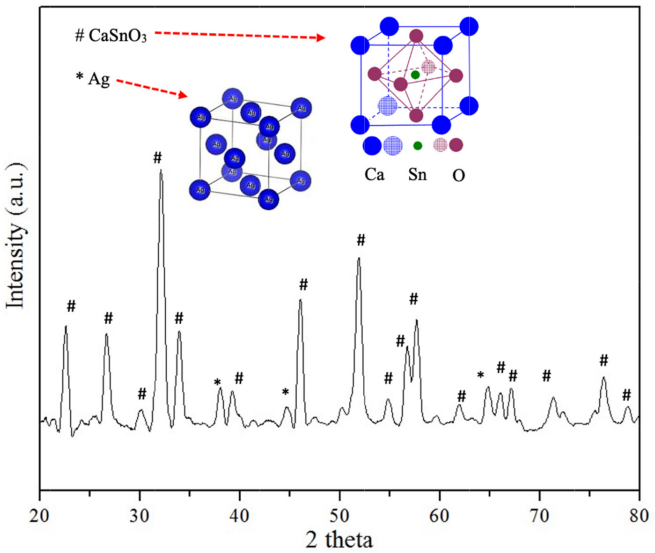

Fig. 2. XRD pattern of the synthesized sample.

wavelength, θ is the diffraction angle, and β is the peak width at half the maximum intensity. By plotting a curve of $\beta cos\theta$ versus $sin\theta$, the crystallite size and lattice strain can be estimated. The slope of the line gives the strain, and the y-intercept gives the crystal size (Fig. 3).

The peaks corresponding to both phases were used to determine these parameters. The average crystallite sizes for calcium stannate and silver were calculated to be approximately 154 and 63 nm, respectively. As is evident, the calcium stannate particles have a larger crystallite size. In hydrothermal synthesis, nucleation and growth are the main mechanisms that determine the size, shape, and crystallinity of the synthesized materials. Nucleation is the initial stage in which small clusters of atoms or molecules form in a supersaturated solution. These clusters act as "seeds" for crystal growth. After nucleation occurs, the clusters grow into larger crystals by adding more atoms or molecules from the surrounding solution. The growth process is influenced by several factors, including temperature, pressure, reactant concentration, and reaction time. The lattice strain for calcium stannate and silver was calculated to be approximately 0.0034 and 0.0045, respectively. It seems that the calcium stannate crystallites have grown more than the silver crystallites, but their lattice strain has decreased more during growth.

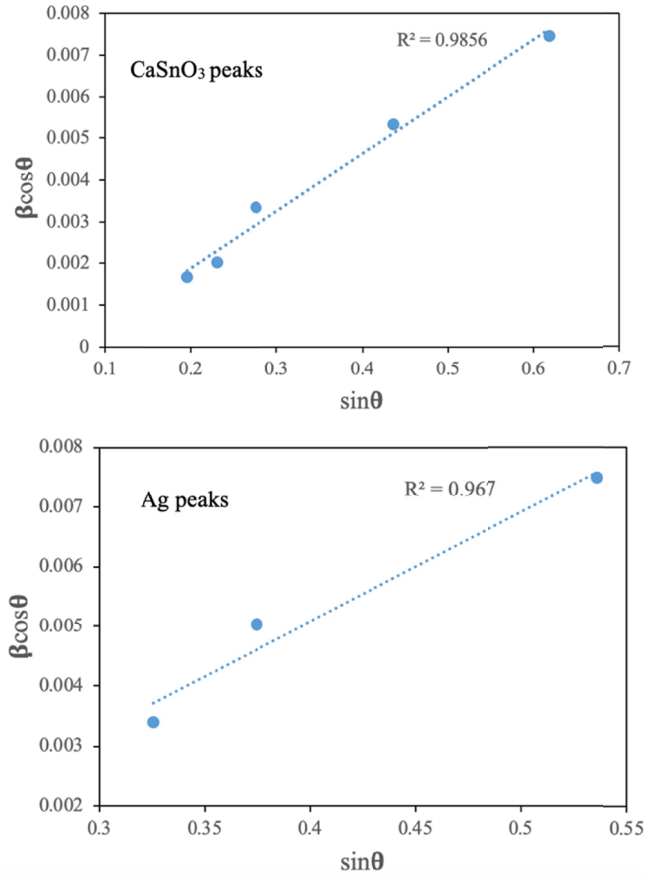

Fig. 3. Williamson-Hall plots of $CaSnO_3$ and Ag peaks.

Fig. 4 shows the scanning electron microscope image and the particle size histogram of the calcium stannate-silver sample.

The microscopic image shows that most of the grains are approximately spherical in shape. Also, the phenomenon of agglomeration is observed in regions of the image due to the high specific surface area of the powders at small dimensions. These particles stick together and form agglomerates to reduce their energy [18]. The particle size histogram shows that the particles have a relatively uniform distribution, and most of them have a grain size between 100 and 250 nm.

Fig. 5 shows the photocatalytic efficiency of pure calcium stannate and calcium stannate-silver samples. As can be seen, the degradation of methyl orange increases with time.

When $CaSnO_3$ was exposed to light, it absorbed photons with energy equal to or greater than its bandgap. This causes electrons in the valence band to be excited to the conduction band, leaving behind holes in the valence band (Eq. (3)).

$$CaSnO_3 + h\nu \rightarrow e_{CB}^{-} + h_{VB}^{+} \quad (3)$$

It was reported that the distorted orthorhombic structure

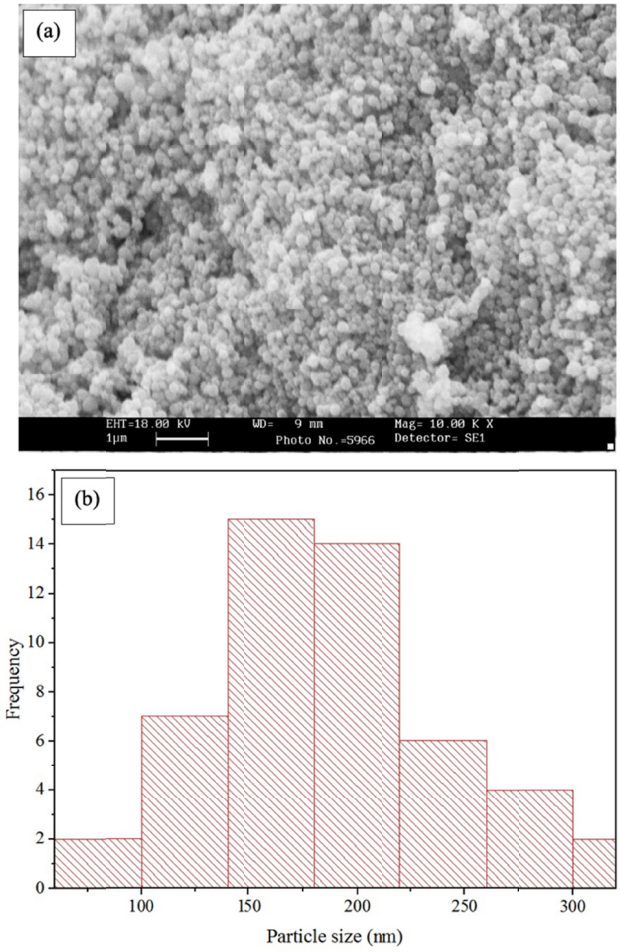

Fig. 4. (a) SEM image, and (b) particle size histogram of the calcium stannate-silver sample.

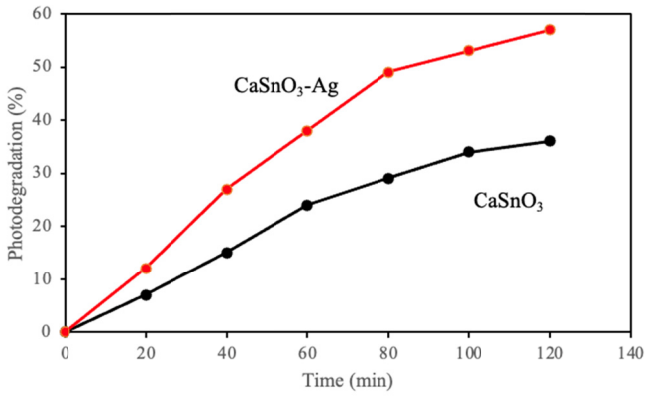

Fig. 5. Photodegradation curve of pure calcium stannate and calcium stannate-silver samples.

of $CaSnO_3$, characterized by tilted SnO_6 octahedra, creates internal dipole fields that enhance charge separation and reduce electron-hole recombination [19]. Then, the photogenerated electrons and holes participate in photodegradation reactions. Electrons reduce oxygen molecules adsorbed on the surface to form superoxide radicals (Eq. (4)).

$$O_2 + e_{CB}^- \rightarrow \cdot O_2^- \quad (4)$$

Holes oxidize water or hydroxide ions to generate hydroxyl radicals (Eq. (5)).

$$H_2O + h_{VB}^+ \rightarrow \cdot OH + H^+ \quad (5)$$

The reactive oxygen species attack and break down organic methyl orange into smaller, less harmful molecules like CO_2 and H_2O.

Also, the composite sample shows higher photocatalytic properties compared to the pure sample. The reason for the higher photocatalytic power of the composite sample can be attributed to the interaction of silver metal and calcium stannate, which causes a reduction in electron-hole recombination. In addition, it was reported that silver can increase light absorption by the surface plasmonic resonance effect [20]. However, more investigation is necessary to determine the dominant photodegradation mechanism of this system.

Kinetic Eq. (6) was used to investigate the kinetic constant of methyl orange photodegradation on pure calcium stannate and calcium-silver stannate [21].

$$Ln(C_0/C) = kt \quad (6)$$

where C_0 is the initial concentration of methyl orange, C is the concentration of methyl orange at time t, and k is the kinetic constant of the degradation reaction. By plotting the curve and determining the slope of the line, the kinetic constant of the methyl orange photodegradation reaction can be estimated (Fig. 6). The obtained kinetic rate constant for the pure calcium stannate and calcium stannate-silver samples was 0.004 and 0.007, respectively. The higher kinetic constant of the composite sample indicates the better photocatalytic performance of this sample. It has been reported that silver improves the photocatalytic properties of semiconductors through several mechanisms. Silver nanoparticles have the property of surface plasmon resonance, which leads to strong absorption of visible light. This property increases the efficiency of light absorption in the semiconductor and improves its photocatalytic activity. In addition, silver nanoparticles can act as electron traps and reduce the recombination rate of electron-hole pairs in the semiconductor. This improves the efficiency of charge separation and transfer, resulting in better photocatalytic performance. Also, the presence of these particles can change the redox potential of the semiconductor, making it more effective in producing reactive oxygen species that are essential for photocatalytic reactions [22,23]

The reusability test was used to examine the stability of the calcium stannate-silver samples (Fig. 7). A standard process involved centrifuging the composite samples, washing them with water, drying them overnight at 80 °C, and then repeating this process four more times. As can be seen, there is a slight drop in their potential photocatalyst efficiency. Repeated use can lead to the aggregation of nanoparticles, reducing their surface area and increasing the recombination rate of charge carriers. This results in lower photocatalytic efficiency. In addition, the surface of photocatalysts can become deactivated due to the accumulation of reaction byproducts. This reduces the availability of active sites for photocatalytic reactions.

4. Conclusion

In the present study, a calcium stannate-silver

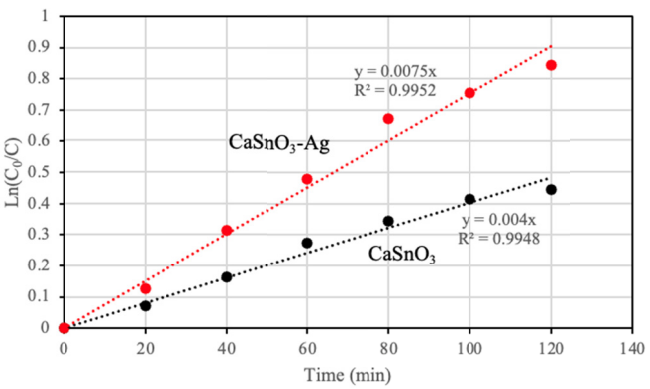

Fig. 6. Degradation kinetic curves of pure calcium stannate and calcium stannate-silver samples.

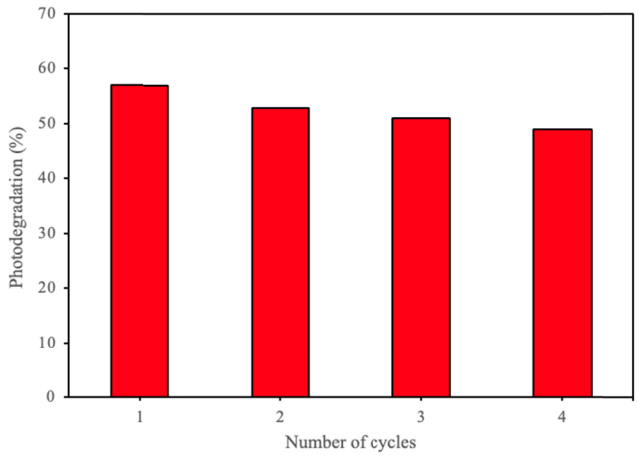

Fig. 7. Recycle tests of the calcium stannate-silver sample.

photocatalyst was fabricated using the hydrothermal method. The produced product was examined in terms of its phases and microstructure. XRD analysis and SEM were used to characterize the samples. The XRD analysis results showed that calcium stannate and silver were successfully formed. The crystallite sizes of calcium stannate were larger than those of the silver phase, while its lattice strain was lower. The produced particles were approximately spherical in shape, and most of the particles were 100 to 250 nm in size. The results of photocatalytic activity showed that this composite has the potential to harness the light better and improve the photodegradation rate of organic dye for use as a promising photocatalyst. However, more investigations should be carried out on the dominant photodegradation mechanisms of this composite system as a photocatalyst.

Disclosure statement

No potential conflict of interest was reported by the author.

References

[1] Aljuaid, A., Almehmadi, M., Alsaiari, A. A., Allahyani, M., Abdulaziz, O., Alsharif, A., Alsaiari, J. A., Saih, M., Alotaibi, R. T., & Khan, I. (2023). g-C3N4 Based Photocatalyst for the Efficient Photodegradation of Toxic Methyl Orange Dye: Recent Modifications and Future Perspectives. *Molecules, 28*(7), 3199. https://doi.org/10.3390/molecules28073199

[2] Kishor, R., Purchase, D., Saratale, G. D., Ferreira, L. F. R., Hussain, C. M., Mulla, S. I., & Bharagava, R. N. (2021). Degradation Mechanism and Toxicity Reduction of Methyl Orange Dye by A Newly Isolated Bacterium *Pseudomonas aeruginosa* MZ520730. *Journal of Water Process Engineering, 43*, 102300. https://doi.org/10.1016/j.jwpe.2021.102300

[3] Azimi-Fouladi, A. Falak, P., & Hassanzadeh-Tabrizi, S. A. (2023). The Photodegradation of Antibiotics on Nano Cubic Spinel Ferrites Photocatalytic Systems: A Review. *Journal of Alloys and Compounds, 961*, 171075. https://doi.org/10.1016/j.jallcom.2023.171075

[4] Borges, M. E., Sierra, M., Cuevas, E., García, R. D., & Esparza, P. (2016). Photocatalysis with Solar Energy: Sunlight-Responsive Photocatalyst Based on TiO_2 Loaded on a Natural Material for Wastewater Treatment. *Solar Energy, 135*, 527-735. https://doi.org/10.1016/j.solener.2016.06.022

[5] Wang, W., Li, G., Xia, D., An, T., Zhao, H., & Wong, P. K. (2017). Photocatalytic Nanomaterials for Solar-Driven Bacterial Inactivation: Recent Progress and Challenges. *Environental Science: Nano,* 4, 782-799. https://doi.org/10.1039/C7EN00063D

[6] Qiu, X., Zhang, Y., Zhu, Y., Long, C., Su, L., Liu, S., & Tang, Z. (2021). Applications of Nanomaterials in Asymmetric Photocatalysis: Recent Progress, Challenges, and Opportunities. *Advanced Materials, 33*(6), 2001731. https://doi.org/10.1002/adma.202001731

[7] Moshtaghi, S., Gholamrezaei, S., & Salavati-Niasari, M. (2017). Nano Cube of $CaSnO_3$: Facile and Green Co-Precipitation Synthesis, Characterization and Photocatalytic Degradation of Dye. *Journal of Molecular Structure, 1134*, 511-519. https://doi.org/10.1016/j.molstruc.2016.12.098

[8] Venkatesh, G., Palanisamy, G., Srinivasan, M., Vignesh, S., Elavarasan, N., Pazhanivel, T., Al-Enizi, A. M., Ubaidullah, M., Karim, A., & Prabu, K. M. (2022). $CaSnO_3$ Coupled g-C_3N_4 S-Scheme Heterostructure Photocatalyst for Efficient Pollutant Degradation. *Diamond and Related Materials, 124*, 108873. https://doi.org/10.1016/j.diamond.2022.108873

[9] Venkatesh, G., Prabhu, S., Geerthana, M., Baskaran, P., Ramesh, R., & Prabu, K. M. (2020). Facile Synthesis of rGO/$CaSnO_3$ Nanocomposite as an Efficient Photocatalyst for the Degradation of Organic Dye. *Optik, 212*, 164716. https://doi.org/10.1016/j.ijleo.2020.164716

[10] Hosseini, M., Ghanbari, M., Dawi, E. A., Alubiady, M. H. S., Al-Ani, A. M., Alkaim, A. F., & Salavati-Niasari, M. (2024). $CaSnO_3$/g-C_3N_4 S-Scheme Heterojunction Photocatalyst for the Elimination of Erythrosine and Eriochrome Black T from Water under Visible Light. *Results in Engineering, 21*, 101903. https://doi.org/10.1016/j.rineng.2024.101903

[11] Li, H., Gao, Y., Gao, D., & Wang, Y. (2019). Effect of Oxide Defect on Photocatalytic Properties of $MSnO_3$ (M= Ca, Sr, and Ba) Photocatalysts. *Applied Catalysis B: Environmental, 243*, 428-437. https://doi.org/10.1016/j.apcatb.2018.10.076

[12] Shah, N. H., Abbas, M., Qasim, M., Sulaman, M., Imran, M., Azmat, S., Cui, Y., & Wang, Y. (2023). Tuning the Catalytic Performance of $CaSnO_3$ by Developing an S-Scheme p–n Heterojunction through $Ag_6Si_2O_7$ Doping. *Catalysis Science & Technology, 13*(22), 6490-6504. https://doi.org/10.1039/D3CY01151H

[13] Rakesh, G. N., Priyadarshini, H. N., Alharethy, F., Pavitra, V., Anusha, B. R., Appu, S., Aarti, D. P., Srinivas Reddy, G., Nagaraju, G., & Prashantha, K. (2024). $CaSnO_3$ Nanorod-Decorated Bi_2WO_6 Nanosheets as a Stable Heterojunction Photocatalyst for Improved Photocatalysis and Nitrite Sensing. *New Journal of Chemistry, 48*(33), 14819-14833. https://doi.org/10.1039/D4NJ01286K

[14] An, C., Wang, S., Sun, Y., Zhang, Q., Zhang, J., Wang, C., & Fang, J. (2016). Plasmonic Silver Incorporated Silver halides for Efficient Photocatalysis. *Journal of Materials Chemistry A, 4*(12), 336-352. https://doi.org/10.1039/C5TA07719B

[15] Bhunia, S. K., & Jana, N. R. (2014). Reduced Graphene Oxide-Silver Nanoparticle Composite as Visible Light Photocatalyst for Degradation of Colorless Endocrine Disruptors. *ACS Applied Materials & Interfaces, 6*(22), 20085-20092. https://doi.org/10.1021/am505677x

[16] Yu, J., Yang, Y., Sun, F., & Chen, J. (2024). Research Status and Prospect of Nano Silver (Ag)-Modified Photocatalytic Materials for Degradation of Organic Pollutants. *Environmental Science and Pollution Research, 31*, 191-214. https://doi.org/10.1007/s11356-023-31166-4

[17] Zak, A. K., Majid, W. H. A., Abrishami, M. E., & Yousefi, R. (2011). X-Ray Analysis of ZnO Nanoparticles by Williamson–Hall and Size-Strain Plot Methods. *Solid State Science, 13*(1), 251-256. https://doi.org/10.1016/j.solidstatesciences.2010.11.024

[18] Pang, W., Li, Y., DeLuca, L. T., Liang, D., Qin, Z., Liu, X., Xu, H., & Fan, X. (2021). Effect of Metal Nanopowders on the Performance of Solid Rocket Propellants: A Review. *Nanomaterials, 11*(10), 2749. https://doi.org/10.3390/nano11102749

[19] Lucena, G. L., de Lima, L. C., Honório, L. M. C., de Oliveira, A. L. M., Tranquilim, R. L., Longo, E., de Souza, A. G., da S. Maia, A., & dos Santos, I. M. G. (2017). $CaSnO_3$ Obtained by Modified Pechini Method Applied in the Photocatalytic Degradation of an Azo Dye. *Cerâmica, 63*, 536-541. https://doi.org/10.1590/0366-69132017633682190

[20] Kumar, R., Janbandhu, S. Y., Sukhadeve, G. K., & Gedam, R. S. (2023). Enhanced Visible-Light Photodegradation of Organic Pollutants by Surface Plasmon Resonance Supported Ag/ZnO Heterostructures. *Journal of Materials Research, 38*(2), 557-570. https://doi.org/10.1557/s43578-022-00844-3

[21] Zawadzki, P., Kudlek, E., & Dudziak, M. (2018). Kinetics of the Photocatalytic Decomposition of Bisphenol a on Modified Photocatalysts. *Journal of Ecological Engineering, 19*(4), 260-268. https://doi.org/10.12911/22998993/89651

[22] Chakhtouna, H., Benzeid, H., Zari, N., Qaiss, A. E. K., & Bouhfid, R. (2021). Recent Progress on Ag/TiO_2 Photocatalysts: Photocatalytic and Bactericidal Behaviors. *Environmental Science and Pollution Research, 28*, 44638-44666. https://doi.org/10.1007/s11356-021-14996-y

[23] Sabry, R. S., Aziz, W. J., & Rahmah, M. I. (2020). Employed Silver Doping to Improved Photocatalytic Properties of ZnO Micro/Nanostructures. *Journal of Inorganic and Organometallic Polymers and Materials, 30*(11), 4533-4543. https://doi.org/10.1007/s10904-020-01661-z

Additional information

Correspondence and requests for materials should be addressed to S. A. Hassanzadeh-Tabrizi.

HOW TO CITE THIS ARTICLE

Hassanzadeh-Tabrizi, S. A.; (2024). Synthesis and investigation of photocatalytic properties of $CaSnO_3$/Ag composite, *J. Part. Sci. Technol. 10(2) 109-115.*

DOI: 10.22104/jpst.2025.7413.1272
URL: https://jpst.irost.ir/article_1544.html